# Crustal structures of the Rhinegraben and the Massif Central grabens: An experimental approach

Laurent Michon, Olivier Merle

TECTONICS, VOL. 19, NO. 5, PAGES 896-904 OCTOBER 2000

# Crustal structures of the Rhinegraben and the Massif Central grabens: An experimental approach

Laurent Michon and Olivier Merle
Laboratoire Magmas et Volcans, Clermont-Ferrand, France

**Abstract** Two of the most important segments of the west European Rift, the Rhinegraben and the Massif Central grabens, show in plan and in cross section a very different crustal structure. The Rhinegraben and the Massif Central grabens are roughly parallel and formed in the same time interval (i.e., Priabonian/Oligocene). The Rhinegraben in the north is a single half graben of ~35 km wide that resulted from the activity of a major detachment fault running from the surface to a MOHO discontinuity at depth. The Massif Central in the south is composed of two lateral half grabens, similar to the Rhinegraben, and a near-symmetric central graben. The opposing detachment faults of the two lateral half grabens reveal a striking mirror symmetry on either side of the symmetric central graben. Experiments have been conducted to explain mechanically this contrasted structural evolution in the same rift system. It is shown that this difference may be attributed to (1) the number of ruptures in the brittle part of the mantle lithosphere and (2) variations in the extension rate. A single rupture in the brittle mantle lithosphere results in either a single half graben or a pair of half and symmetric grabens in low and high extension rate experiments, respectively. Two ruptures in the brittle mantle lithosphere result in two half grabens in low rate experiments. The number of grabens is dependent upon the distance between the two ruptures in the brittle mantle lithosphere in high extension rate experiments and may vary from 2 to 4. Estimation of the extension rate in the Rhinegraben and the Massif Central matches experimental results and shows that the strength ratio between lower and brittle crust is the key parameter in determining the graben geometry.

## 1. Introduction

Understanding of the geometry of sedimentary basins associated with rifting processes in the continental lithosphere has made great progress over the past 10 years [e.g., *Allemand and Brun*, 1991; *Buck*, 1991; *Benes and Davy*, 1996; *Scholz and Contreras*, 1998]. Despite this progress, the process of graben initiation is still controversial. Because reflection seismic studies clearly show that some extensional structures are asymmetric at the graben scale as revealed for the Rhinegraben [*Brun et al.*, 1991], the Malawi rift [*Rosendhal et al.*, 1992], or the Basin and Range province [*Allimendinger et al.*, 1983], it is widely considered that the passive rifting may be induced by a lithospheric asymmetric simple shear [*Wernicke*, 1985; *Brun and Beslier*, 1996]. However, several authors also propose that the initial stage of a passive margin evolution may be explained by a pure shear evolution at lithospheric scale [*Keen and Dehler*, 1993].

The aim of this paper is to determine, using scaled models, graben geometry during continental passive rifting. According to many authors [e.g., *Buck*, 1991; *Davy and Cobbold*, 1991; *Burg et al.*, 1994; *Allemand and Brun*, 1991], we assume that the continental lithosphere is characterized by a four-layer strength profile with two brittle high strength layers (the upper crust and the upper mantle lithosphere) and two ductile layers (the lower crust and the lower mantle lithosphere). As a result of such a lithospheric strength profile, it has been shown that crustal deformation is largely controlled by ruptures within the brittle mantle lithosphere [*Beslier*, 1991; *Brun and Beslier*, 1996].

In the present paper, we examine at crustal scale the graben geometry resulting from the failure of the brittle mantle lithosphere. As known from geomechanics, the strength of a viscous material is dependant on the strain rate, so that the rate of extension is supposed to be of paramount importance in the graben geometry. We study the influence of different parameters such as the variation of the strength ratio between the upper and the lower crust or the number of ruptures in the underlying mantle.

Experimental results explain mechanically why a single rupture in the brittle mantle may induce the formation of either a unique asymmetric graben or two parallel, symmetric and asymmetric, grabens. Our model also emphasizes the importance of the rate of extension upon the graben geometry in the crust. Finally, the experimental models may explain the differences depicted in the west European Rift between the Massif Central grabens and the Rhinegraben geometries.

## 2. Experimental Background

### 2.1. Scaling

Analogue modeling of crustal deformation is similar to nature if experimental models and natural systems are characterized by a similar distribution of stresses, densities, and rheologies [*Hubbert*, 1937]. The continental lithosphere with a normal thermal gradient is considered as a four-layer model for which the deformation is initiated from the failure of the brittle mantle [*Beslier*, 1991]. As a mantle lithospheric rupture occurs, the resulting crustal structure is highly dependent on the mechanical coupling between the brittle and ductile part of the crust. This brittle/ductile coupling can be estimated from the strength ratio between the upper and lower crust [*Allemand*, 1990; *Beslier*, 1991; *Benes and Davy*, 1996; *Brun*, 1999]. We use this strength



Paper number 2000TC900015.
0278-7407/00/2000TC900015$12.00

ratio to achieve similarities between nature and experiments. This ratio is a dimensionless number that must be of the same order of magnitude in model and nature.

$$\left(\frac{S_B}{S_D}\right)_{\text{Model}} = \left(\frac{S_B}{S_D}\right)_{\text{Nature}}. \quad (1)$$

The strength $S_B$ of a brittle material corresponds to the deviatoric stress $\sigma_1$-$\sigma_3$ (where $\sigma_1$ and $\sigma_3$ are the maximum and minimum principal stresses, respectively), which increases linearly with depth $h$ and fluctuates as a function of the density $\rho$, the angle of friction $\phi$, the gravity acceleration $g$, and the cohesion $\tau_0$ ((2)-(4)). It follows for a divergent tectonic regime

$$\sigma_1 = a + b\sigma_3 = \rho g h, \quad (2)$$

$$a = 2\tau_0\sqrt{b}, \quad (3)$$

$$b = \frac{1+\sin\phi}{1-\sin\phi}. \quad (4)$$

In the upper crust the average density $\rho_n$ is ~2700 kg m$^{-3}$ (continental crust with an overall granitic composition), the cohesion is ~$10^7$ Pa, and the angle of friction is close to 30°. These natural values make it possible to determine the strength $S_B$ of the brittle upper part of the crust. In experiments where cohesionless material is used the strength of the upper brittle part simplifies to

$$S_B = \sigma_1 - \sigma_3 = \frac{2}{3}\rho g h. \quad (5)$$

In the lower ductile layer the strength $S_D$ is dependant on the viscosity $\mu$ and the strain rate $\varepsilon$, which may be calculated from the ratio between the extension rate $V$ and the thickness of the ductile layer $h_D$.

$$S_D = \mu\frac{V}{h_D}. \quad (6)$$

Then, the strength ratio may be estimated both in nature and experiments. In experiments it simplifies to

$$\frac{S_B}{S_D} = \frac{\frac{2}{3}\rho g h}{\mu\varepsilon}. \quad (7)$$

In our experiments the brittle upper crust is made of sand, which is a cohesionless material [*Davison et al.*, 1993] with a density $\rho_m$ of ~1400 kg m$^{-3}$. The length scale ratio is $10^{-6}$, so that 1 cm in the model represents 10 km in nature. The angle of friction $\phi$, being a dimensionless number, must be similar in nature and experiments ($\phi_{sand}$=30° and $\phi_{nature}$=30°). We use a silicone with a viscosity $\mu_m$=3x10$^4$ Pa s to simulate a lower crust with a viscosity of ~ $\mu_n$=$10^{21}$ Pa s.

The experiments are an attempt to understand the mechanisms of crustal deformation in an overall slight extension of a few tens kilometers (10/30 km) within a time interval of ~10 million years. The strain rate in nature ranges from $10^{-15}$ to $10^{-16}$ s$^{-1}$. In order to achieve in experiments a strength ratio similar to that inferred in nature (a few tens to a few hundred) the extension rate in experiments varies from 0.15 to 1.4 cm h$^{-1}$, which yields a strength ratio in experiments ranging from 4.5 to 130.

### 2.2. Apparatus

The experimental model is 50 cm long and 3 cm thick and is made of a brittle upper part and a ductile lower part. The brittle upper part is composed of alternating horizontal sand layers of different colors used as passive markers. The ductile lower part is a homogeneous pink silicone in most experiments. However, we have also used vertically and horizontally stratified silicone in order to determine the internal strain in the ductile level, following an experimental procedure already proposed and explained in detail by some authors [*Dixon*, 1974; *Merle*, 1982; *Brun and Merle*, 1985; *Allemand*, 1990]. The basal plate of the model simulates the boundary between the crust and the brittle mantle. As in the experiments of *Basile and Brun* [1999] the rupture within the brittle mantle, which is considered to govern crustal deformation, is achieved by a velocity discontinuity (VD) long the basal plate (Figure 1). In the end of the experiment the brittle material is wetted, and serial cross sections, perpendicular to the strike of the grabens, make it possible to analyze the geometry and the internal strain recorded in the model.

We have conducted two sets of experiments, which differ in the VD number. The first set was carried out with a single VD (one-velocity discontinuity model). The model is limited by a motionless wall on one side and by a mobile rim that is pulled out with the mean of a screw jack on the other side (Figure 2a). A plastic sheet underlying half of the model is attached to the mobile rim. The limit of the plastic sheet, which is underneath the silicone and parallel to the mobile rim, induces a VD in the middle central part of the model during motion. The second set of experiments was carried out with two VD (two-velocity

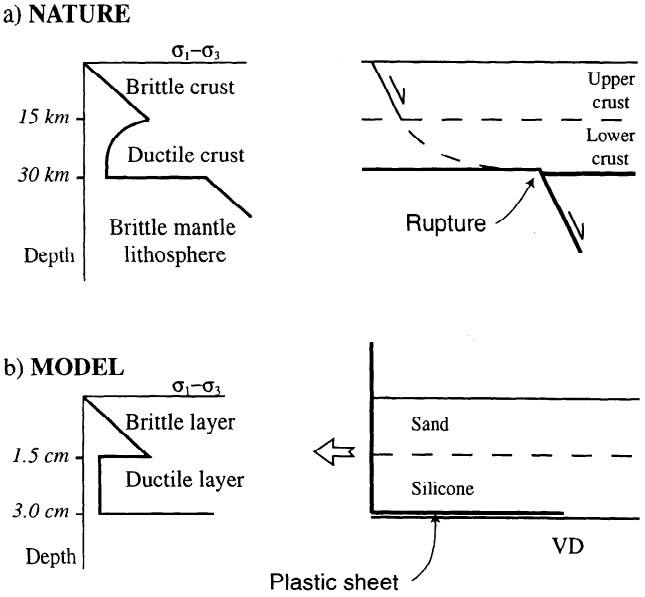


**Figure 1.** Strength profile in (a) nature and (b) experiments. The velocity discontinuity resulting from failure within the brittle mantle in nature is modeled in experiments by the rim of a mobile plastic sheet at the base of the model.

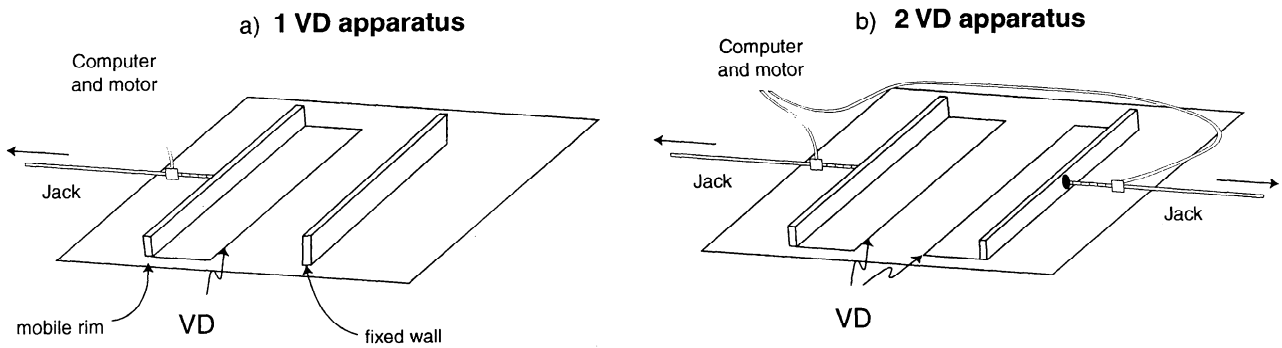


**Figure 2.** Experimental devices for (a) one-velocity discontinuity models and (b) two-velocity discontinuities models.

discontinuity model). The former motionless wall is replaced by a mobile rim to which is attached a second plastic sheet (Figure 2b). During each experiment the velocity of each mobile rim is achieved by a step by step motor controlled by a computer.

## 3. One-Velocity Discontinuity Model

The goal of these experiments is to study the geometry and the deformation mechanisms associated with the activity of a single VD. The strength ratio is dependent upon both the extension rate and the ratio of thickness between the brittle and the ductile part of the model. We have conducted several experiments with the same amount of extension and the same thickness ratio in order to determine the role of the extension rate on the graben geometry. Then, varying the velocity of the mobile wall makes the strength ratio to change from 4.5 to 130 and the role of the extension rate in the graben geometry needs to be determined.

### 3.1. Influence of the Strength Ratio

In experiments with a strength ratio <65-70 the extension initiates two linear and parallel grabens: a near-symmetric one located above the motionless part of the model and an asymmetric one located above the movable plastic sheet. The latter half graben presents a well-pronounced asymmetry with a major detachment fault facing the symmetric graben (Figure 3a). This overall geometry does not differ when varying the strength ratio from 4.5 to 65-70. Experiments with identical strength ratios allow one to define two constants $C_a$ and $C_b$. The constant $C_a$ is the width of the symmetric graben. For instance, $C_a$ is ~2 cm for a strength ratio of ~25. The constant $C_b$ is the distance between the center of the symmetric graben and the master detachment fault of the asymmetric graben. $C_b$ is ~8 cm for a strength ratio of 25. However, the constant $C_b$ slightly increases with time owing to the displacement of the half graben onto the movable plastic sheet. The constant $C_b$ is also related to the strength ratio as it may increase (up to 1 cm) when increasing this ratio.

In experiments with a strength ratio >70 the extension generates a unique and asymmetric graben on the movable part (Figure 3b). On map view this half graben is linear and parallel to the rims of the model. In cross section the half graben is very similar to that observed in low strength ratio experiments, having the same width and the same orientation for the detachment fault. This result indicates that a high strength ratio prevents the formation of the symmetric companion graben observed in low strength ratio experiments.

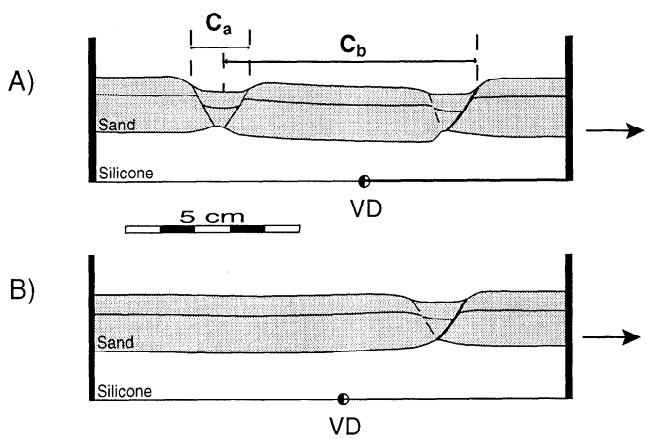


**Figure 3.** Two cross sections in one-velocity discontinuity experiments for (a) low strength ratio and (b) high strength ratio. The constant $C_a$ is defined as the width of the symmetric graben, and $C_b$ is defined as the final distance between the center of the symmetric graben and the master fault of the half graben.

### 3.2. Internal Strain in the Ductile Lower Part

In some experiments, along strike, half of the silicone is stratified vertically, whereas the second half is stratified horizontally. The width and the thickness of the vertical and horizontal layers are identical, so that a deformed grid is obtained by superposition of two cross sections in the horizontally and vertically stratified halves of the model after deformation (a complete description of this experimental procedure is given by *Brun and Merle*, [1985]). This allows one to fully define the strain pattern within the ductile lower part of the model during extension.

In experiments with a strength ratio equal to 24, cross sections reveal that the strain (1) can be slightly different along strike in the same experiment, (2) is due to major low-angle high-strain zones dipping ~25°-30°, and (3) is mainly localized between the two grabens (Figure 4). Cross sections allow two sets of nearly symmetric high-strain zones to be determined. First, two high-strain zones are arranged in a more or less pronounced mirror

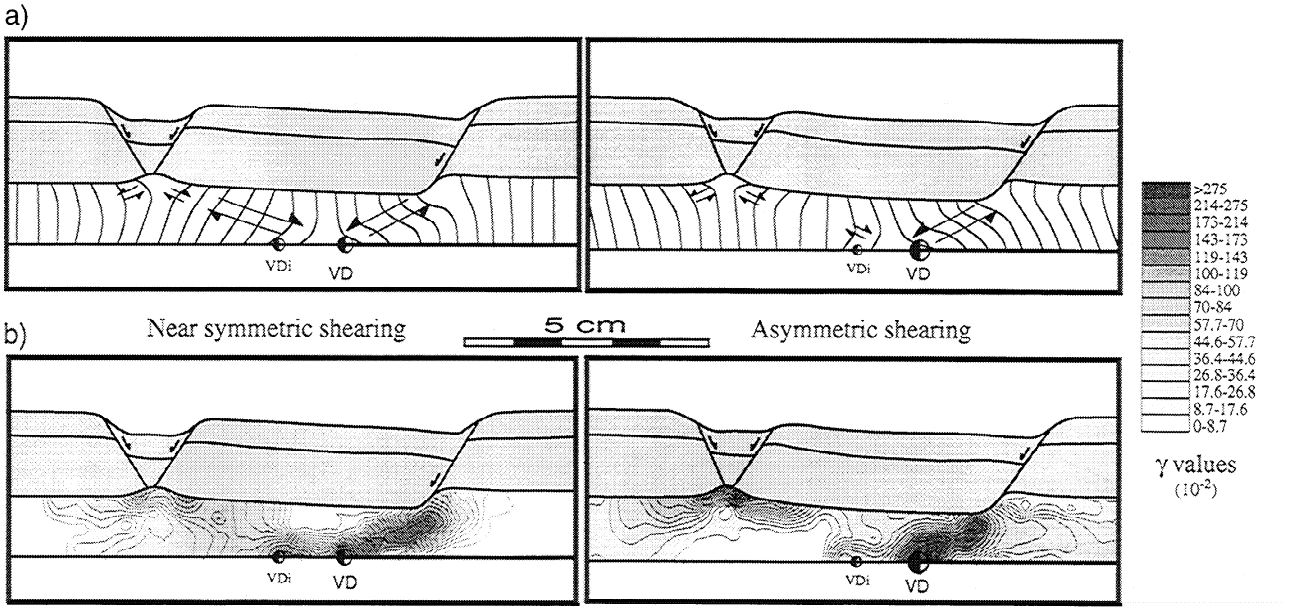


**Figure 4.** Cross sections in one-velocity discontinuity experiments showing the final shape of (a) initially vertical markers and (b) shear magnitudes in the lower ductile layer.

symmetry on both sides of the velocity discontinuity. The two high-strain zones intersect at depth between the initial ($VD_i$) and final position (VD) of the velocity discontinuity. The high-strain zone associated with the detachment fault of the half graben affects the entire thickness of the silicone layer in all experiments. Shear measurements $\gamma$ reveal that the highest strain values are recorded along it (Figure 4b). It is also well worth noting that the brittle block in between the two grabens is slightly tilted according to the activity of the main detachment fault of the half graben. Second, two high-strain zones are localized below the symmetric graben on either side of its central axis and are restricted to the very upper part of the silicone layer.

This strain analysis shows that the prominent feature of the deformation in such an extensional process is the detachment fault of the half graben along which very high strain is recorded in the lower ductile part. We argue that extension with high strength ratio, which inhibits the formation of the symmetric graben, would be mainly characterized by a single major high strain-zone running from the bottom of the brittle fault in the sand to the velocity discontinuity at depth.

## 4. Two-Velocity Discontinuities Model

In experiments with a low strength ratio (<65-70) the overall geometry can be understood as a function of the initial distance between the two velocity discontinuities (Figure 5). As the initial distance between the two velocity discontinuities is superior to 6 cm (for a strength ratio equal to 18), each VD induces the formation of a pair of grabens in a way similar to that described for a low strength ratio in one-VD experiments (Figure 5a). Increasing the initial distance between the two VD makes the distance between the two pairs of graben (i.e., the central horst) increase.

In experiments with an initial distance equal to 5±1 cm, extension leads to the formation of three grabens only: two lateral half grabens and a central symmetric one (Figure 5b). The distance between this unique central graben and the two other lateral half grabens is identical to the distance between each pair

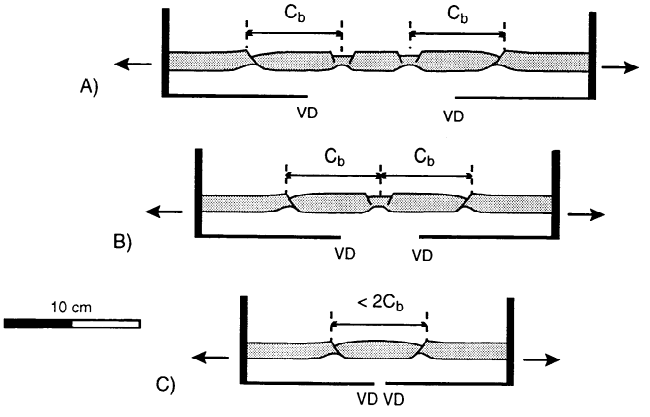


**Figure 5.** Schematic representation of extensional structures in two-velocity discontinuities and low strength ratio experiments. When the starting distance between the two VD is large, each VD initiates a pair of half graben/symmetric graben as in one-VD low strength ratio experiments (Figure 5a). A larger starting distance between the two VD merely increases the width of the central horst between the two pairs of grabens linked to each VD. When the starting distance between the two VD is reduced, a single symmetric graben is shared by the two half grabens as the distance between those two is not enough to create two symmetric grabens (Figure 5b). When the two VD are touching or are very close, the distance between the two border faults becomes too short for creating a symmetric graben, and the two half grabens are separated by a central horst (Figure 5c).

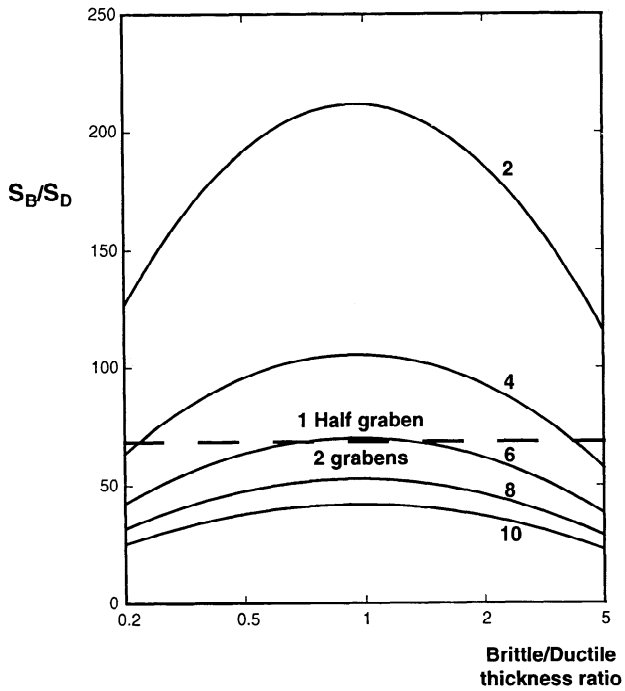


**Figure 6.** Strength ratio versus brittle/ductile thickness ratio for five different extension rates: 2, 4, 6, 8, and 10 $10^{-11}$ m $s^{-1}$ (see text for explanation).

of associated grabens (i.e., constant $C_b$) in previous experiments. We propose that the distance between the two half grabens being too small for two symmetric grabens to form, a single central graben develops and is shared by the two lateral half grabens.

Finally, with an initial distance inferior to 4 cm the system is restricted to the formation of the two lateral half grabens. The distance between the half grabens is smaller than the constant $C_b$, which probably prevents the formation of any symmetric graben in between (Figure 5c).

In experiments with a high strength ratio (>70) the extension always induces the formation of two half grabens, whatever the initial distance between the two velocity discontinuities. This result is consistent with high strength ratio one-VD experiments.

## 5. Discussion

It is interesting to analyze the influence of the thickness of the brittle upper part of the crust on the strength ratio. Computations show that the strength ratio reaches a maximum for a thickness ratio of 1, decreasing to zero as the thickness ratio tends both to zero and infinity (Figure 6). At high extension rate the thickness ratio has no effect on the number of grabens, and extension leads to the formation of two, symmetric and asymmetric, grabens. In contrast, at low extension rate a thickness ratio in the range from 0.2 to 5 may induce the formation of a single half graben (Figure 6).

In nature the thickness ratio may fluctuate from 0.5 to 2 according to the geothermal gradient within the crust at the time of the deformation. Considering these two end-members, Figure 7 shows that the strength ratio is more sensitive to changes in extension rate than to variations in thickness ratio. No matter what the thickness ratio is, an extension rate higher or lower than ~$6x10^{-11}$ m $s^{-1}$ leads to the formation of a single half graben or of a pair of grabens, respectively (Figure 7). We conclude that the extension rate is the main parameter controlling the graben geometry in nature.

As the strength ratio is <65-70 (i.e., relatively high extension rate), the initial stage of the deformation in one-VD experiments is associated with the formation of two symmetric high-strain zones in the silicone layer. In the brittle layer these high-strain zones lead to the formation of two grabens. As the extension increases, the graben located on the mobile part becomes asymmetric, whereas the other remains symmetric. The shear zone related to the symmetric graben becomes less and less active whereas, high shear strain is recorded along the major shear zone related to the half graben. These results can be usefully compared with the experiments of *Brun and Beslier* [1996, Figure 4b] at lithospheric scale where the symmetric graben becomes progressively inactive with time and where the deformation is concentrated in the asymmetric one. The one-VD experiments with a strength ratio >65-70 (i.e., relatively low extension rate) show that the extension induces from the beginning a major high-strain zone, which leads to the formation of a single half graben in the brittle layer.

These experiments make it possible to assess in nature the role of the distance between the rupture zones in the brittle mantle with respect to the extension rate. In two-VD experiments with a strength ratio >65-70 (i.e., low extension rate) the extension always leads to the formation of two asymmetric grabens. This shows that the overall geometry at low extension rate is not controlled by the initial distance between the VD and that each rupture in the brittle mantle generates an half graben in the overlying crust. However, low strength ratio experiments (i.e., high extension rate) reveal that the geometry and the number of graben are controlled by the initial distance between the two VD (Figure 8).

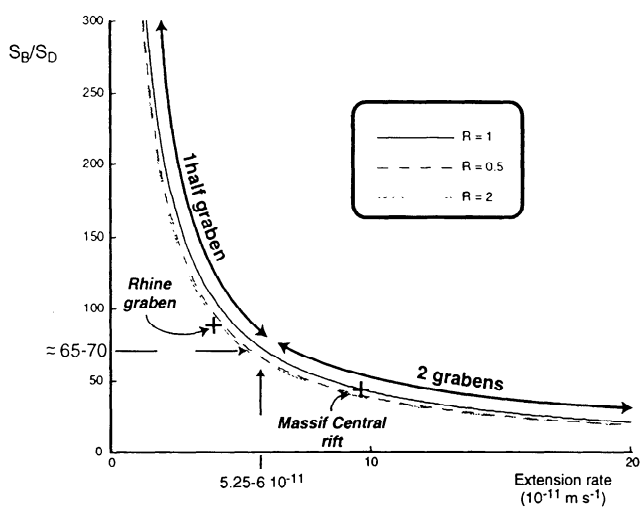


**Figure 7.** Strength ratio versus extension rate for three different brittle/ductile thickness ratios. The Rhinegraben plots in the single half graben field, whereas the Massif Central plots in the two grabens field.

| | | High extension rate | Low extension rate |
|---|---|---|---|
| 1 VD | | 2 grabens | 1 graben |
| 2 VD | 0<d<4 | 2 grabens | 2 grabens |
| | 4<d<6 | 3 grabens | |
| | d>6 | 4 grabens | |

**Figure 8.** Table showing the number of grabens with respect to the number of velocity discontinuities and the extension rate. Here $d$ (cm) is the initial distance between two velocity discontinuities.

According to the length ratio, an initial distance between the two mantle lithospheric ruptures >60 km, that is, for a distance between the two lateral detachment faults >160 km (2 $C_b$), should generate two pairs of grabens in nature, each symmetric/asymmetric pair being induced by the rupture in the underlying brittle mantle. The width of the two symmetric central grabens would be ~20 km. In contrast, as the initial distance between the two ruptures is <40 km, that is, where the distance between the two lateral detachment faults is <2 $C_b$, only two half grabens should form because the distance between them is not large enough for the symmetric graben to be initiated. Finally, between these two end-members a particular case may be defined for which a central graben of 20 km width is shared by the two lateral half grabens. This geometry would occur where the two lithospheric ruptures are 50±10 km apart.

## 6. A Natural Example: The West European Rift

The west European Cenozoic rift is composed of three principal segments whose orientation is roughly parallel to the alpine front: the Eger graben in the east and the Rhinegraben and the Massif Central grabens in the west (Figure 9) [Ziegler, 1994]. Numerous seismic profiles [e.g., *Morange et al.*, 1971; *Bergerat et al.*, 1990; *Brun et al.*, 1991; *Zeyen et al.*, 1997] together with well-established geological data have unraveled the tectonic history and helped to visualize the crustal structure for the Rhinegraben and the Massif Central grabens.

### 6.1. Rhinegraben

The Rhinegraben is a 35-40 km wide and 300 km long linear structure which is NNE-SSW oriented and results from a near E-W extension. Geophysical data clearly show that the graben presents an asymmetry which is reversed from north to south. North to the Lalaye-Lubine-Baden-Baden Variscan fault the graben is bounded in the east by a west dipping major fault. South to the Variscan fault the main fault is east dipping, and the thickest sediment deposit is localized in the western part (Figure 10a). The Rhinegraben results from a lithospheric extension which started 40 myr ago. Between 40 and 30 Ma the evolution of the northern and southern parts was identical with a sedimentation at sea level [*Sissingh*, 1998] and similar subsidence rates [*Villemin et al.*, 1986]. From the end of the Oligocene the evolution of the southern and northern parts differed. In the south

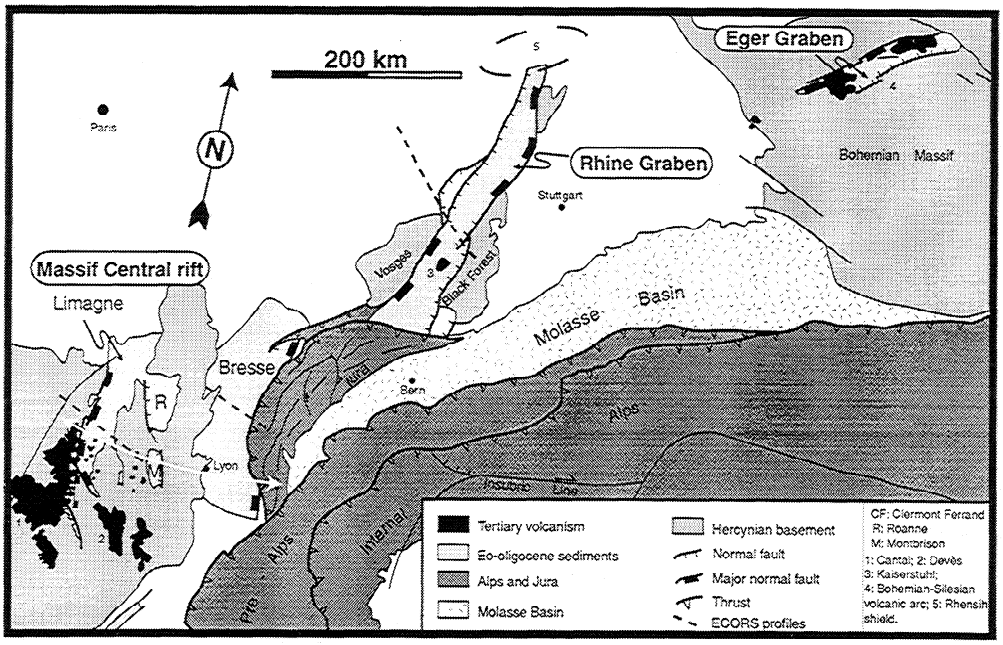


**Figure 9.** Geological map of the three main segments (Massif Central, Rhine, and Eger) of the west European Rift. Also shown is the location of the E-W cross section of the Massif Central (white arrow) and the three geophysical profiles including the ECORS profile in the Rhinegraben (dashed lines).

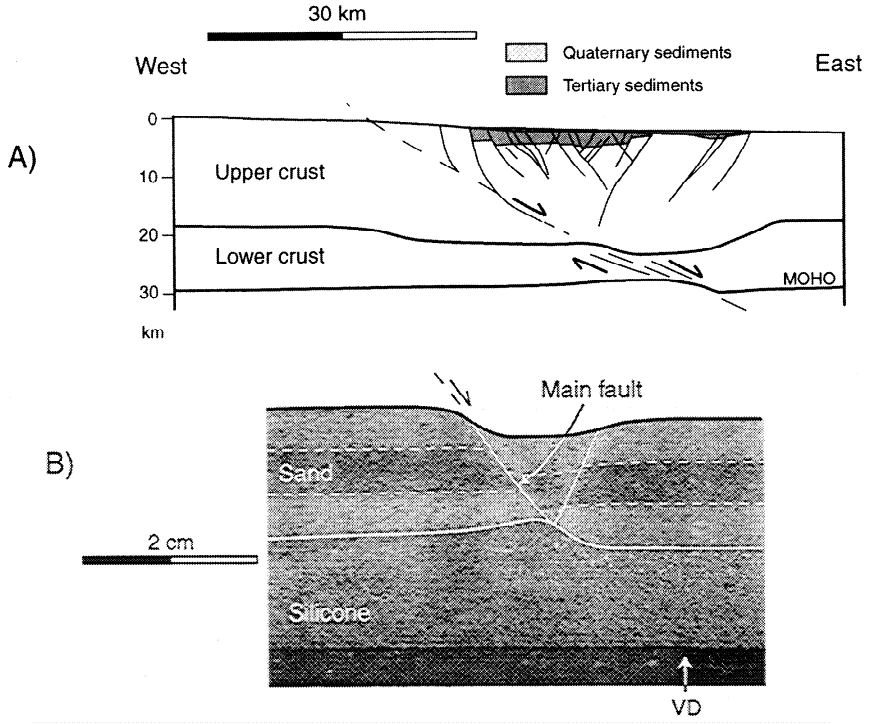


**Figure 10.** (a) The graben geometry of the southern part of the Rhinegraben as deduced from the ECORS profile shown on Figure 9 [modified after *Brun et al.*, 1992]. (b) Cross section in one-VD high strength ratio experiments. The half graben is bounded by a detachment fault from the surface to the velocity discontinuity at depth.

the subsidence drastically decreased, while it has continued to present in the northern part. The thickness of sediments and the crustal thinning is therefore larger in the northern than in the southern part. The sedimentation at sea level and the lack of volcanism during the rifting episode are considered as strong arguments to interpret the Rhinegraben in terms of passive rather than active rifting [e.g., *Park*, 1988; *Ruppel*, 1995].

The upper crustal stretching in the northern part deduced from the sedimentary fill is estimated between 5 and 7 km. Assuming a preservation of the volume of the crust, a total extension value of ~17 km can be estimated [*Brun et al.*, 1992]. This crustal stretching in the northern part results, on one hand, from the extension linked to the west European rift (between 40 and 30 Ma) and, on the other hand, from the Plio-Quaternary extension. This latter extensional episode is closely connected with the recent evolution of the Rhur and the southern North Sea graben [*Zijerveld et al.*, 1992; *Kooi et al.*, 1992]. In order to determine the stretching of the crust induced by the west European rift episode only, it is better to use the stretching value obtained in the southern part (12 km) [*Bois*, 1993].

The extension rate deduced for the 10 Myr Oligocene rifting episode in the southern part is close to $3.8 \times 10^{-11}$ m $s^{-1}$. From seismic profiles the brittle/ductile thickness ratio is ~2 [*Brun et al.*, 1992]. Equations (2)-(6) allow one to calculate a strength ratio of ~88 for the southern Rhinegraben at that time. The strength ratio and the extension rate for the Rhinegraben are shown in the Figure 7. The corresponding point plots in the single half graben field.

As predicted by our experiments, the Rhinegraben geometry presents strong similarities with the half graben obtained in the high strength ratio one-VD experiments (Figure 10b). In nature and experiments the graben is bounded by a main detachment fault, and the maximum of subsidence is situated at the footstep of this fault. In experiments, many conjugate faults are created which migrate toward the graben center. In nature the first faults to be formed would be the external faults, whereas internal faults are late. We speculate that the east-dipping detachment fault remains active while many tilted blocs were formed eastward.

Experiments strongly suggest that each part of the Rhinegraben (southern and northern parts) results from a single rupture within the brittle mantle lithosphere. The Lalaye-Lubine-Baden-Baden fault is then interpreted as a transfer fault which linked the two ruptures in the brittle mantle.

### 6.2. The Massif Central Grabens

The Massif Central area, which is the most important segment of the west European Cenozoic rift, has been recently reinterpreted [*Merle et al.*, 1998]. The Eo-Oligocene graben structure is 180 km wide, composed of two lateral half grabens (the Limagne graben in the west and the Bresse graben in the east) and one near-symmetric, 20 km wide, central graben (the Roanne-Montbrison graben) (Figure 11a). The overall structure along an east-west cross section is bounded by the two opposing detachment faults of Limagne and Bresse lateral grabens and reveals a striking mirror symmetry on either side of the central part of the Roanne-Montbrison graben.

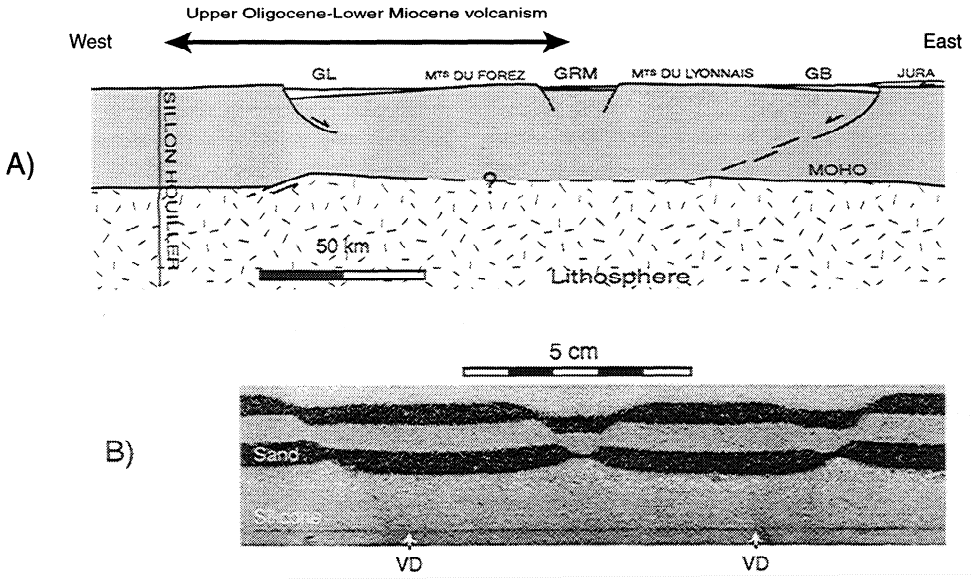


**Figure 11.** (a) The graben geometry of the Massif Central, which corresponds to a mirror symmetry on either side of an axis passing through the center of the central symmetric graben. The overall geometry results from upper Eocene/lower Oligocene extension. The necking of the crust revealed by seismic studies below the Limagne graben is thought to result from a late extensional stage in the upper Oligocene (see text). GL, Limagne graben; GRM, Roanne-Montbrison graben; GB, Bresse graben. (b) Cross section from a two-VD low strength ratio with an initial distance of ~5 cm between the two VD showing a similar overall symmetry. According to length scale ratio, the 20 km wide central graben in nature fits the 2 cm wide central graben in experiments.

The Massif Central grabens result from an east-west extension which lasted 10 Ma in the Oligocene time and during which each graben was filled by several hundred or thousand meters of sediments. During lower and middle Oligocene, marine incursions show that the sedimentation occurred at sea level in the Limagne and Bresse grabens [*Giraud*, 1902; *Rat*, 1984; *Bodergat et al.*, 1999], while fluvio-lacustrian sedimentation only was recorded in the central graben of Roanne-Montbrison [*Ech-Cherif El Kettani*, 1996]. In the upper Oligocene this overall symmetry came to an halt. Persistence of marine incursions and sedimentation in the Limagne graben together with a lull in sediment deposits in the Roanne-Montbrison and Bresse grabens suggests that the extension became asymmetric at the scale of the whole system. During this period, crustal thinning only occurred in the western Limagne graben. This is clearly visible on geophysical profiles where crustal thinning reaches 25% in the Limagne graben whereas, it does not exceed 11% in other grabens.

We argue that the extensional process in the upper Oligocene differs from that recorded in the lower and middle Oligocene, during which the mirror symmetry of the grabens system were initiated. The more pronounced crustal and lithospheric thinning due to the upper Oligocene extension along the western part of the system is confirmed by the occurrence, from the end of the Oligocene and during lower Miocene, of a scattered volcanic phase mainly located within the Limagne graben and totally missing to the east of the Roanne-Montbrison graben (Figure 11a). As in the Rhinegraben the sedimentation at sea level, which lacks volcanic activity and was followed by a scattered volcanic phase in the thinned area, may be interpreted in terms of passive rifting evolution [*Merle et al.*, 1998].

The stretching value in the upper crust may be estimated from master fault geometries to be inferior to 10-15 km. As in the Rhinegraben this value is smaller than that deduced from geophysical data, which is close to 25-30 km. Again, this discrepancy can be explained by ductile flow in the lower crust during extension. Equations (2)-(4) and (6) allow an estimation of the strength ratio which ranges from 39 to 47. In contrast with the Rhinegraben, the corresponding point plots in the two grabens field on Figure 7. This strongly suggests that the whole geometry of the massif central grabens may be interpreted in terms of two-VD experiments.

Accordingly, the Massif Central grabens could result from two ruptures in the brittle mantle underlying the ductile crust. Low strength ratio would have induced the near-symmetric central graben, which is shared by the two lateral half grabens in a way similar to our experiments (Figure 5b). From the length ratio used in experiments it may be inferred that these two ruptures in the underlying brittle mantle are spaced by ~50 km (Figure 11b). Reactivation of former variscan faults could explain the distance between the two border faults (Bresse and Limagne detachment faults), which is slightly superior to that observed in experiments.

## 7. Conclusions

The main results of this experimental study may be summarized as follows.

1. As already proposed by some authors [e.g., *Allemand*, 1990;

*Beslier*, 1991; *Benes and Davy*, 1996), crustal-scale experiments show that the strength ratio is the key parameter which controls the geometry of the graben in rifting processes. In one-VD experiments a strength ratio value of ~65-70 (i.e., yield strength ratio) separates two deformation fields. Lower and higher strength ratio values induce either a pair of grabens or a single asymmetric graben, respectively. In two-VD experiments the extension leads to the formation of two asymmetric grabens as the strength ratio is higher than the yield strength ratio. For a strength ratio lower than the yield value the geometry and the number of grabens is a function of the initial distance between the two VD (Figure 5 and 8).

2. Variations of the thickness ratio between the brittle and ductile part of the crust have little influence on the strength ratio value, which is extremely sensitive to extension rate variations. The extension rate during extension is therefore a parameter of paramount importance in the understanding of the graben geometry.

3. Analogue modeling allows interpretation of the difference in the graben geometry observed in the Rhine and Massif Central areas. It may be inferred that the overall geometry results from (1) the number of ruptures within the brittle mantle lithosphere and (2) the difference in the extension rate. Two relatively close ruptures in the underlying brittle lithosphere as well as a high extension rate explain that three grabens formed in the Massif Central, whereas a unique rupture in the lithosphere and a low extension rate explain that a single half graben formed in the Rhine area.

**Acknowledgments.** The authors want to thank Dick Nieuwland and François Roure for their critical reviews and Pascal Allemand for a very constructive discussion.

## References


Allemand, P., Approche expérimentale de la mécanique du rifting continental, *Mem. Doc. Geosci. Rennes*, 38, 175 p., 1990.

Allemand, P., and J.P. Brun, Width of continental rifts and rheological layering of the lithosphere, *Tectonophysics*, *188*, 63-69, 1991.

Allimendinger, R., J.W. Sharp, D. Von Tish, D. Serpa, L. Brown, S. Kaufman, J. Oliver, and R.B. Smith, Cenozoic and Mesozoic structure of the eastern Basin and Range from COCORP seismic reflection data, *Geology*, *11*, 532-536, 1983.

Basile, C., and J.P. Brun, Transtensional faulting patterns ranging from pull-apart basins to transform continental margins: An experimental investigation, *J. Struct. Geol.*, *21*, 23-37, 1999.

Benes, V., and P. Davy, Modes of continental lithospheric extension: Experimental verification of strain localisation processes, *Tectonophysics*, *254*, 69-87, 1996.

Bergerat, F., J.L. Mugnier, S. Guellec, C. Truffert, M. Cazes, B. Damotte, and F. Roure, Extensional tectonics and subsidence of the Bresse basin: An interpretation from ECORS data, *Mem. Soc. Geol. Fr.*, *156*, 145-156, 1990.

Beslier, M.O., Formation des marges passives et remontée du manteau: Modélisation expérimentale et exemple de la marge de la Galice, *Mem. Doc Geosci Rennes*, *45*, 199p., 1991

Bodergat, A.M., D. Briot, M. Hugueney, J.L. Poidevin, L. Picot, F. Giraud, J.P. Berger, A Levy, and A Poignant, Incursions marines dans l'environnement lacustre du rift oligocène de Limagne (Massif Central, France): Apport des organismes halophiles et des isotopes du strontium; datations par les mammifères, *Bull Soc. Geol. Fr*, *170*, 499-511, 1999.

Bois, C, Initiation and evolution of the Oligo-Miocene rift basins of Southwestern Europe: Contribution of deep seismic reflection profiling, *Tectonophysics*, *226*, 227-252, 1993.

Brun, J.P., Narrow rifts versus wide rifts: Inferences for the mechanics of rifting from laboratory experiments, *Philos. Trans. R. Soc. London, Serv. A*, *357*, 695-712, 1999.

Brun, J.P, and M.O. Beslier, Mantle exhumation at passive margin, *Earth Planet Sci. Lett.*, *142*, 161-173, 1996.

Brun, J P., and O. Merle, Strain patterns in models of spreading-gliding nappes, *Tectonics*, *4*, *7*, 705-719, 1985.

Brun, J.P., F. Wenzel, and ECORS-DEKORP team, Crustal scale structure of the Southern Rhinegraben from ECORS-DEKORP seismic reflection data, *Geology*, *19*, 758-762, 1991.

Brun, J.P., M.A. Gutscher, and DEKORP-ECORS teams, Deep crustal structure of the Rhine Graben from DEKORP-ECORS seismic reflection data: A summary, *Tectonophysics*, *208*, 139-147,1992.

Buck, R., Modes of continental lithospheric extension, *J. Geophys. Res.*, *96*, 20,161-20,178, 1991

Burg, J.P., P. Davy, and J. Martinod, Shortening of analogue models of the continental lithosphere: New hypothesis for the formation of the Tibetan Plateau, *Tectonics*, *13*, 475-483, 1994.

Davison, I., M. Insley, M. Harper, P. Weston, D. Blundell, K. McClay, and A. Quallington, Physical modelling of overburden deformation around salt diapirs, *Tectonophysics*, *228*, 255-274, 1993.

Davy, P., and P.R. Cobbold, P.R., Experiments on shortening of 4-layer continental lithosphere, *Tectonophysics*, *188*, 1-25, 1991.

Dixon, J.M., A new method of determining finite strain in models of geological structures, *Tectonophysics*, *24*, 99-114, 1974.

Ech-Cherif El Kettani, D., Géologie du fossé du Forez: Essai de synthèse et comparaison avec les autres bassins tertiaires du Massif Central français, *Ph.D. thesis, Univ. of St Etienne, St Etienne, France*, 1996.

Giraud, J., Etudes géologiques sur la Limagne (Auvergne), *Thèse d'Etat, Ed. Ch. Béranger, Paris*, 410p., 1902.

Hubbert, K.M., Theory of scale models as applied to the study of geologic structures, *Geol. Soc. Am. Bull.*, *48*, 1459-1520, 1937.

Keen, C.E., and S.A. Dehler, Stretching and subsidence: Rifting of conjugate margins in the North Atlantic Region, *Tectonics*, *12*, 1209-1229, 1993.

Kooi, H., M. Hettema, and S. Cloetingh, Lithospheric dynamics and the rapid Pliocene-Quaternary subsidence phase in the Southern North Sea Basin, *Tectonophysics*, *192*, 245-259, 1991.

Merle, O., Cinématique et déformation de la nappe du Parpaillon, *Ph.D. thesis, Univ. of Rennes, Rennes, France*, 1982.

Merle, O., L. Michon, G. Camus, and A. Goër, L'extension oligocène sur la transversale septentrionale du rift du Massif central, *Bull. Soc. Geol. Fr.*, *169*, 615-626, 1998.

Morange, A., F. Heritier, and J. Villemin, Contribution de l'exploration pétrolière à la connaissance structurale et sédimentaire de la Limagne, dans le Massif Central, *Symposium J. Jung. Plein Air Service, Clermont Ferrand*, 295-308, 1971.

Park, R.G., Geological structures and moving plates, *Blackie & Son Ltd, Bishopbriggs, Glasgow*, 337p, 1988.

Rat, P., Une approche de l'environnement structural et morphologique du Pliocène et du Quaternaire bressan, *Géol. Fr.*, *3*, 185-196, 1984.

Rosendhal, B.R., E. Kilembe, and K. Kaczmarick, Comparison of the Tanganyika, Malawi, Rukwa and Turkana Rift zones from analyses of seismic reflection data, *Tectonophysics*, *213*, 235-256, 1992.

Ruppel, C., Extensional processes in continental lithosphere, *J. Geophys. Res.*, *100*, 24,187-24,215, 1995.

Scholz, C.H., and J.C. Contreras, Mechanics of continental rift architecture. *Geology*, *26*, 967-970, 1998

Sissingh, W., Comparative Tertiary stratigraphy of the Rhine Graben, Bresse Graben and Molasse Basin: Correlation of Alpine foreland events, *Tectonophysics*, *300*, 249-284, 1998.

Villemin, T., F. Alvarez, and J. Angelier, The Rhinegraben. Extension, subsidence and shoulder uplift, *Tectonophysics*, 128, 47-59, 1986.

Wernicke, B., Uniform-sense normal simple shear of the continental lithosphere, *Can. J. Earth Sci.*, *22*, 108-125, 1985

Zeyen, H., O. Novak, M. Landes, C. Prodehl, L. Driard, and A. Hirn, Refraction-seismic investigations of the northern Massif Central (France), *Tectonophysics*, *275*, 99-117, 1997.

Ziegler, P.A., Cenozoic rift system of western and central Europe: An overview, *Geol. Mijnbouw*, *73*, 99-127, 1994.

Zijerveld, L., R. Stephenson, S Cloetingh, E. Duin, and M.W. Van Den Berg, Subsidence analysis and modelling of the Roer Valley Graben (SE Netherlands), *Tectonophysics*, *208*, 159-171, 1992.


O. Merle and L. Michon, Laboratoire Magmas et Volcans, 5 rue Kessler, 63038 Clermont-Ferrand Cedex, France, (michon@opgc.univ-bpclermont.fr)

(Received December 9, 1999;
revised May 3, 2000;
accepted May 9, 2000.)